



Experimental study and test of a new biosorbent prepared from bean peels to remove Rhodamine B from industrial wastewaters

Naima Gherbi*, Zakarya Ziani, Mokhtar Khetib, Djanet Belkharchouche, Abdeslam-Hassen Meniai

Laboratoire de l'Ingénierie des Procédés de l'Environnement, Université Constantine 3 Salah Boubnider, Algeria, emails: naima.gherbi@univ-constantine3.dz (N. Gherbi), zakiziani92@gmail.com (Z. Ziani), mkhetib1@gmail.com (M. Khetib), belnadjat@yahoo.fr (D. Belkharchouche), meniai@yahoo.fr (A.-H. Meniai)

Received 11 April 2020; Accepted 20 January 2021

ABSTRACT

Bean peels solid wastes are present in abundance, with no evident use and with no cost, hence their application as a new biosorbent to remove Rhodamine B (RhB) from wastewaters effluents from the textile industry. This was motivated by the performance achieved by many natural solid compounds when used as biosorbents, particularly in the removal of organic and inorganic pollutants mainly from industrial, agriculture, and even household wastewaters. The effects of different parameters on the adsorbent capacity, such as the contact time, the adsorbent dose (1–20 g/L), and the initial concentration of RhB (2–1,000 mg/L), initial pH (2–12) were investigated. The results showed that the retention process was rapid and the adsorption equilibrium could be reached after 25 min with an adsorbent dose of 10 g/L. The highest Rhodamine removal efficiency value was 99.16% for a high concentration of 1,000 mg/L. Equilibrium adsorption results followed the Freundlich isotherm, whereas the experimental kinetics data were best fitted to the pseudo-second-order equation. Finally, the obtained results confirm that bean peels had a large capacity of adsorption, making it an effective and economical biosorbent to remove RhB from wastewaters.

Keywords: Bean peels; Rhodamine B; Adsorption; Textile industry; Wastewaters; Depollution; Dyes

1. Introduction

Water resources are still facing severe pollutions due to industrial and even domestic activities, despite the fact that it is essential for sustaining all forms of life, food production, economic development, general well-being, etc., and it is not easy to find substitutes for most of its uses [1].

In fact, most of the water pollution is due to human activities, mainly industrial ones which are responsible for the release of huge masses of polluting species into the environment, contaminating rivers, watercourses, and even groundwaters.

One of the industrial fields that release important quantities of polluting species is the textile industry which is a great user of dyes. More than 100 tons of dyes are released per year into the environment and contaminate rivers, watercourses, etc. [2], mainly due to the dyeing processes where the lost dye percentage may reach up to 50% because of low levels of dye-fiber fixation [3]. Moreover, the generated wastewaters are characterized by the presence of organics with intense colors [3], high biological oxygen demand/chemical oxygen demand (BOD/COD) [4], and wide variation in pH [5]. Some of these industrial textile wastes are highly toxic and carcinogenic to humans

* Corresponding author.

and animals [2] with high toxicity levels as confirmed by the current tests such as those of daphnia Magna [6,7]. These were the main factors that motivated the present study, focussing on the elimination of dyes released into the environment, by the textile industry.

In fact, dyes are chemically stable compounds and highly persistent in the environment and therefore they are regarded as a major potential source for environmental contamination [8]. They must imperatively be removed from industrial effluents to mainly prevent the soil and the groundwaters pollution. Several treatment techniques and processes such as coagulation [2], flocculation, advanced oxidation processes (Fenton oxidation), ozonation [7], heterogeneous photo-catalytic oxidation (PCO) [9], electrocoagulation [10], membrane filtration, and adsorption [11], have been used to treat industrial aqueous effluents in order to remove dyes mainly released by the textile industry. However, as reported in the literature [12,13], each method has advantages and disadvantages like for instance the advanced oxidation processes which can achieve an effective wastewaters decolorization but lead to sludge generation, or the ozonation which is characterized by a no change in the effluent volume but also disadvantageously by a short half-life of about 20 min. The photo-chemical-based technique does not generate any sludge but gives the chance to by-products formation whereas an electrochemical-based method does not show hazardous end products but its major constraint is a high electricity cost. Regarding sorption based processes, the adsorption onto activated carbon is effectively highly performing for various dyes. However, it remains a very expensive process, contrary to adsorption onto peat which has proven to be a good adsorbent due to its cellular structure but its specific surface area is relatively low. Similarly, cucurbituril has shown a good sorption capacity for dyes but it is also highly costly. Surely other techniques with advantages and disadvantages for the removal of dyes from textile industries do exist and a compromise should be reached in most cases.

In fact, adsorption is one of the simplest, most used, and efficient techniques for the removal of pollutants soluble in industrial wastewater effluents [14], but its main constraint is the high cost of activated carbon. This has encouraged the extensive study of biomaterials like household and agricultural wastes with respect to the adsorption process. This has been mainly motivated by their composition consisting of certain materials like lipids, proteins, hemicelluloses, lignin, simple sugars, hydrocarbons, and starch providing functional groups presenting a good affinity with various species like organic or inorganic pollutants, leading to performing biosorbents with high retention capacities [14]. Many research works have focussed on the enhancement of these biosorbents retention capacity by means of pretreatment techniques like washing, chemical treatment, drying, grinding, etc. This would be in favor of sustainable development, valorizing solid wastes, and contributing to remove pollution, preserving the environment [15]. In fact in the literature, the use of various bio-adsorbents which are greatly available and with low or no cost, has been discussed in details and presented as a good alternative to expensive traditional adsorbents like activated carbon, citing several examples like nut shell, apple skin, orange peel,

dates kernels, olive kernels, peach stones, banana peel, grenadine peels, and pod beans, etc. [16].

The objective of the present study was to test the retention capacity of prepared solid support from bean peel as adsorbent to eliminate a model dye pollutant, Rhodamine B (RhB) which is highly water-soluble [17] and is extensively used in printing, painting, leather, and textile industries as well as a well-known fluorescent water tracer. It is characterized by a more rigid structure than other organic dyes [18]. Due to its high toxicity, RhB may be harmful to humans and animals, affecting the respiratory tracts [19], the reproductive and nervous systems and subcutaneous tissue bone sarcoma when present in drinking water [18], as well as causing skin irritations [19].

2. Experimental procedure

2.1. Material

Bean peels were collected locally and washed with distilled water to eliminate any impurities and dried in sunlight, before sieving to get small size particles which underwent a further washing to eliminate water-soluble substances, then they were dried at 110°C up to a constant weight. The final material was then ground, sieved to obtain particles with diameter <0.160 mm, and kept in the desiccator ready for use.

RhB ($C_{28}H_{31}ClN_2O_3$) was supplied as a green or red to violet powder by BIOCHEM (chemophara). It is a macromolecular compound with the following molecular structure shown in Fig. 1 and reported in [20].

2.2. Methods

2.2.1. Fourier transform infrared spectroscopy

In order to identify the surface chemical functions of the support, Fourier transform infrared (FTIR) analyses were carried out using JASCO FT/IR spectrometer (Jasco, UK). The samples were mixed thoroughly with potassium bromide at 1:10 (sample: potassium bromide) weight ratio after being ground. Scans were obtained at a resolution of 4 cm^{-1} , from 4,000 to 400 cm^{-1} .

2.2.2. Porosity characterization

The characterization of the porous texture of support was performed using physical adsorption of N_2 at 77 K using an ASAP 2010 apparatus.

2.2.3. pH_{pzc}

The point of zero charge pH_{pzc} above which the total surface of the adsorbent was negatively charged, was measured by the JENWAY pH-meter type 3510 apparatus (Cole-Parmer, UK). The procedure has been described in details in [21].

2.2.4. Titration

In order to understand the influence of the pH on the RhB retention, it is necessary to consider the acid-base properties at the solid surface and particularly to quantify

the protons H^+ and hydroxides OH^- . This is achieved by a titration method consisting of determining the quantities of both ionic species by a gradual addition of known quantities of appropriate titrating reagents such as nitric acid HNO_3 (0.1 M) and/or sodium hydroxide $NaOH$ (0.1 M) to a given sample, up to the equivalence point.

Comparisons of the obtained titration curves of the mixture of 0.5 g of solid support in 50 mL of 0.01 M of sodium nitrate $NaNO_3$ solution using HNO_3 0.1 M and/or $NaOH$ 0.1 M, were performed. The use of $NaNO_3$ was to keep the ionic strength constant as suggested in Marnier et al. [22,23]. The pH and electrical conductivity were measured using a JENWAY pH-meter (Cole-Parmer, UK). In order to stabilize the pH, the mixture suspension was continuously shaken for 2–5 min, between every two consecutive additions of the acid or the base. The obtained curves are shown in Fig. 5a.

2.2.5. Batch adsorption experiments for removal of dye

The adsorption experiments were carried out batch-wise at an ambient temperature of $20^\circ C \pm 2^\circ C$, in 450 mL Erlen Meyer flasks, keeping the total volume of the reaction mixture at 300 mL and ensuring a continuous agitation at a speed of 200 rpm during a contact time varying from 0 to 180 min. The amount of BP, the concentrations of selected dyes, and the pH of solution, were varied from 1 to 20 g/L, from 2 to 1,000 mg/L, and from 2 to 12, respectively. The resulting suspension was then centrifuged at 5,000 rpm during 10 min. The final solution was analyzed using a UV/visible spectrophotometer (UV-1601 SHIMADZU, Gemini BV, France). The calibration curves were obtained by plotting the absorbance of every single dye against dye concentration at the fixed wavelength (554 nm) as shown in Fig. 2. It is clear that the optical density varies linearly with RhB concentration according to Beer–Lambert law in the considered concentration range. The amount Q (mg/g) of dye adsorbed onto solid was calculated through a mass balance follows:

$$Q \left(\frac{mg}{g} \right) = \frac{C_0 - C_e}{r} \quad (1)$$

where C_0 and C_e are the concentrations (mg/L) of RhB solution before and after adsorption, respectively, and r is the solid/liquid ratio of bean peels.

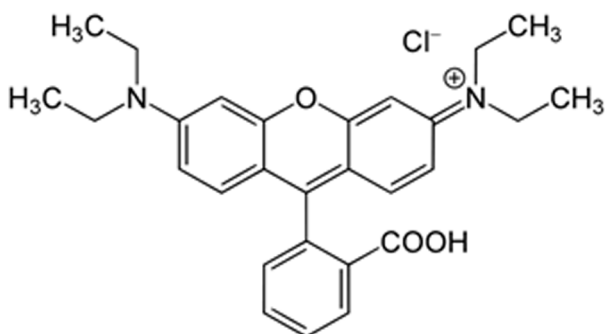


Fig. 1. Rhodamine B dye [19].

3. Results and discussion

3.1. Characterization of bean peels

The obtained IR spectrum showed the presence of several groups such as for instance the bands 3,300 and 2,925 cm^{-1} and other intense bands around 1,616 and 1,013 cm^{-1} that characterize intense strong and elongation attribution C–H, CH_2 , O–NO, and C–O, respectively [24].

Fig. 3 shows The N_2 adsorption/desorption isotherms for BP as in between type II and IV, with a hysteresis loop typical of a mesoporous material [25]. Brunauer–Emmett–Teller (BET) surface and total pore volume were measured and shown in Table 1.

Fig. 4 shows the plot of pH_{final} vs. $pH_{initial}$ of BP and the point zero charge pH_{pzc} was found equal to 6.2 which is close to neutrality, indicating cationic adsorption is favored when pH is greater than 6.2 while adsorption of anions are enhanced at pH less than 6.2 [26].

3.2. Thermal analysis

Table 2 shows the results of BP reactivity in air and N_2 by thermogravimetric analysis (TGA), using a flowrate of 100 mL/min.

These results indicate that the percentage of carbon was very low in this cellulosic precursor, suggesting the use of BP without an activation process.

3.3. Titration

The shape of the titration curve shown in Fig. 5a indicates that BP surface had an amphoteric character, accepting exchanges both with H^+ and OH^- ions at the same time, but with different capacities. This is illustrated by the net difference between the slopes of the curves for the two cases of $NaNO_3$ with and without the presence of BP support. However, quantitatively this can be determined using saturation curves.

The concentrations of the sites are deduced from the titration curves shown in Figs. 5b and c by comparison of $NaNO_3$ salt solution with and without the presence of the solid support (BP). The sorbed $[H^+]$ or $[OH^-]$ quantities at saturation are estimated as follows:

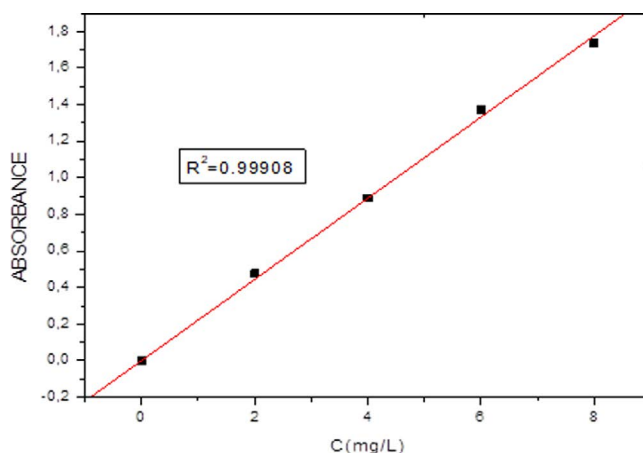


Fig. 2. Calibration curves of RhB.

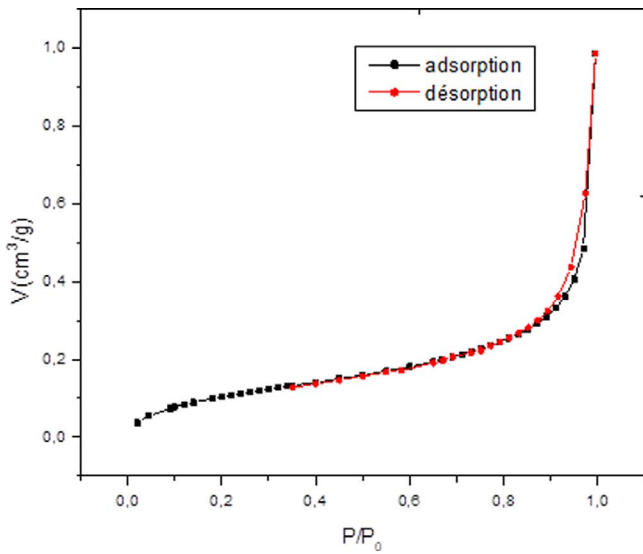


Fig. 3. Adsorption/desorption isotherm for N₂ at 77 K of BP.

Table 1
Characteristics of bean peels

Parameter	Values
BET surface area	0.4213 m ² /g
Pore volume	1.523 × 10 ⁻³ cm ³ /g

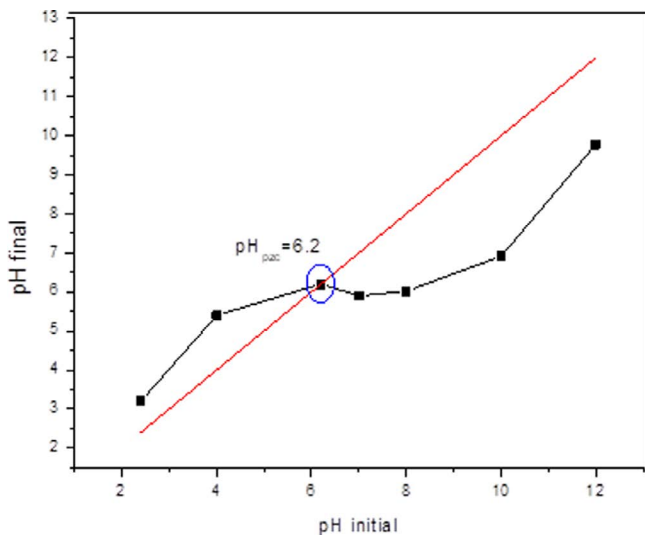


Fig. 4. Plot of pH_{pzc} of BP.

[H⁺] sorbed at saturation = [H⁺] added at saturation – [H⁺] present at saturation
 [OH⁻] sorbed at saturation = [OH⁻] added at saturation – [OH⁻] present at saturation
 The results are:

[H⁺] sorbed at saturation = 2.76 × 10⁻⁴ mol/L
 (0.0276 meq/g of support)

Table 2
Thermal analysis of BP by TGA

Sample	Moisture	Volatiles	Fixed carbon	Ash
BP	8.7%	69.9%	15.5%	5.9%

[OH⁻] sorbed at saturation = 1.39 × 10⁻⁴ mol/L
 (0.0139 meq/g of support)

These results suggest an amphoteric nature of the surface of BP, but more precisely, it can be seen that it tends to be saturated with ions (H⁺) or in general with cations, almost twice as much as for (OH⁻) or with anions.

The total concentration of available surface sites [SOH] is calculated as follows [22]:

$$[SOH] = \frac{[H^+]_{sat} + [OH^-]_{sat}}{2} \quad (2)$$

[SOH] = 2.075 × 10⁻⁴ mol/L; this value comparing with alumina (7.7 × 10⁻⁴ mol/L), kaolinite (1.3 × 10⁻⁴ mol/L) [27], hematite (5.2 × 10⁻⁵ mol/L), and Goethite (4.5 × 10⁻⁵ mol/L) [28] may consider the surface of BP as polar nature [29].

3.4. Effect of solid/liquid ratio on equilibrium adsorption capacity and removal efficiency

The curves showing the variation of the retention capacity with time for the three solid/liquid ratio values of 10, 12, and 15 g/L exhibited two phases: the first one during 30 min was rapid and the second one was independent of time where a sort of saturation was reached with constant retention capacity values of 4.25, 3.75, and 3.1 mg/g, respectively. This can be explained by the fact that the solute molecules might find it difficult to reach vacant sites in the solid adsorbent due to a possible adsorbent surface coverage by the solute molecules. It was also observed that the increase in the solid/liquid ratio led to a decrease in the adsorption capacity Q_e and this might be due to the decrease in the total sorption surface area available to RhB [30] resulting from overlapping or aggregation of sorption sites [31]. Similar behavior for the effect of adsorbent dosage on the dye adsorption capacity was observed and discussed for different types of adsorbents in the literature [32] considering the optimal adsorbent dose of 10 g/L.

Fig. 6 shows the plot between the %R removals against adsorbent dose, the adsorbent dose interval was extended from 1 to 20 g/L. From Fig. 6, it was noted that the BP is effective for all interval of solid–liquid ratio.

Also, it is clear from Fig. 6, that when the adsorbent dose increased the adsorption capacity (adsorbed amount per unit mass of adsorbent) decreased. This may be due to the increasing number of adsorption sites giving the chance for some of them to remain unsaturated or even vacant. This may also be explained by interactions between particles, particularly at high concentrations, forming aggregations which may lead to a decrease of the mass transfer area, an increase in the length of the diffusional path, and desorption of the solute particles weakly bound to the adsorbent surface.

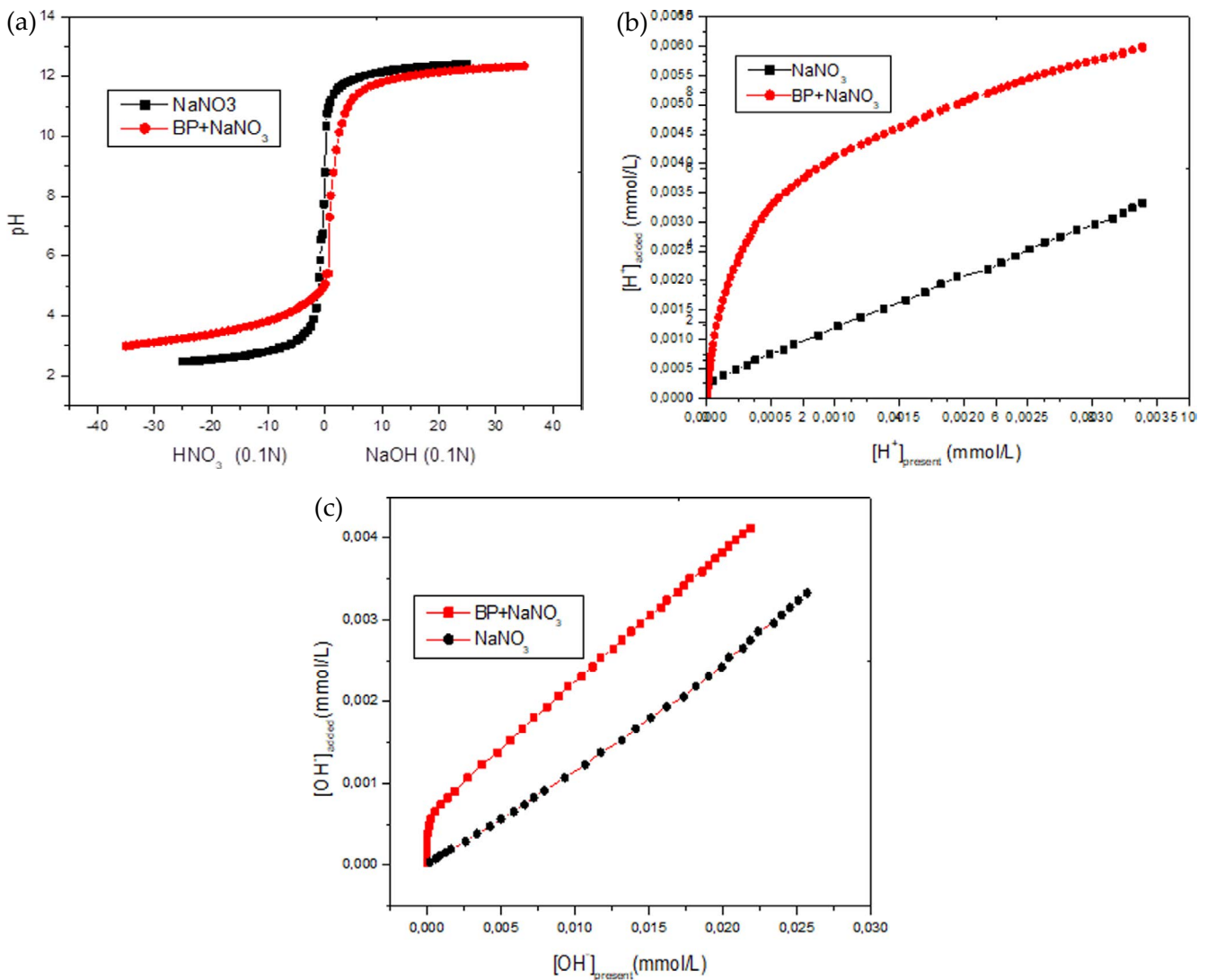


Fig. 5. (a) Experimental titration curve of 0.5 g of solid in 50 cm³ of NaNO₃. Saturation curve of the support surface by (b) H⁺ and (c) OH⁻.

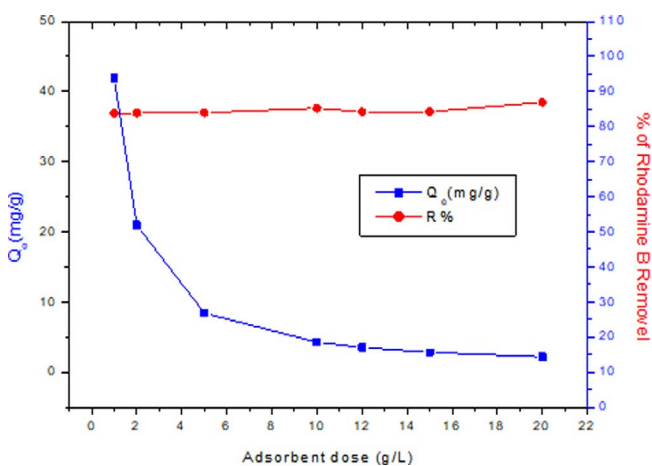


Fig. 6. Effect adsorbent dose on equilibrium adsorption capacity and removal efficiency.

3.5. Effect of initial concentration on kinetics and adsorbed quantity

The initial concentration of the pollutant is also an important parameter for determining the capacity of the substrate. In order to study its effect, arbitrary values of 25, 50, 100, 200, and 400 mg/L were considered. The results indicated that the increase in the initial concentration led to an increase in adsorption capacity. In changing the initial concentration of the RhB solution from 25 to 400 mg/L, the adsorbed amount increased from 2.18 to 39.16 mg/g, corresponding to a removal efficiency varying from 86.14% to 97.82%, respectively. This can be explained by the fact that when the initial concentrations increased, the mass transfer driving force became larger and the interaction between RB and BP was enhanced, hence resulting in higher adsorption capacity. Similar trends are reported by Marmier et al. [27], Khalighi Sheshdeh et al. [32], and Ali and Muhammad [33] for Crystal violet (CV)

removal by adsorption onto almond waste and *Calotropis procera*, respectively. Also similarly to the effect of the adsorbent dose, at a given initial concentration and after a 30 min first phase, the retention capacity reached the equilibrium value and remained constant independently of time. This can be explained by a possible monolayer coverage formation of solute molecules at the adsorbent surface.

The concentration range was varied from 2 to 1,000 mg/L, since the results had confirmed that the equilibrium time was not dependent on the initial concentration. Fig. 7 shows that the change in the adsorbed amount as a function of the initial concentration was linear, and the removal efficiency reached 99.16% for an initial concentration of 1,000 mg/L at high initial concentration of RhB provided the necessary driving force for RhB to overcome the mass transfer resistances between the aqueous phase and BP and 99.9% for 1,000 mg/L indicating that BP was a good adsorbent, contrary to what found in Vieira et al. [2] and Senthil Kumar et al. [34] where the adsorption efficiency of Congo red and Methylene Blue removal decreased with the increase of the initial concentration.

3.6. Influence of pH on RhB removal

The structure of RhB species showed to be influenced by the pH [35,36]. At a strong acidic medium of pH less than 3, positively charged species, RhB-H⁺ and RhB-H₂²⁺ are dominant. At pH greater than 7.0, the neutral zwitterion, RB[±], was partly formed and became predominant in the alkali medium [37,38].

In order to examine the influence of pH on the RhB removal percentage (*R*%), two concentrations of 50 and 400 mg/L were considered and the initial pH of the solution varied from 2 to 12, with still the stirring speed, the temperature, and the solid-liquid ratio kept constant. Fig. 8a shows that the effect of pH was negligible particularly for high initial concentrations (400 mg/L) and remained constant at 98.2%, a value in agreement with that reported in Namasivayam and Yamuna [39]. For low concentration (50 mg/L), the same results were observed, except for pH of 2 and 12 there was a small decrease in

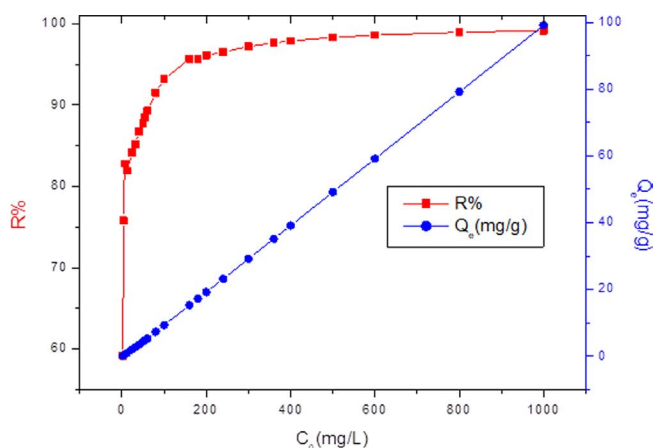


Fig. 7. Effect of initial concentration on adsorbed amount and removal efficiency at equilibrium time.

the removal efficiency. This is a similar result to the one reported in the literature concerning the removal of RhB onto a parthenium biosorbent [40]. To better understand this, the final pH values of the RhB solutions obtained after the adsorption process were also measured as shown in Fig. 8b and indicated that when the pH fluctuated from an acidic value of 3 to a basic one 10, the concentrations of H⁺ and OH⁻ changed accordingly and might be in excess with respect to the number of adsorption sites for which they would be in competition with the RhB molecules, hence influencing the adsorption yield which might change slightly or even remain constant. However, in many research works the pH effect on the solute removal was important, mainly depending on the adsorbent surface properties [41,42].

This is in accordance with the result of the BP surface titration. Therefore, it can be concluded that the surface of the considered support acted as a buffer solution, explaining the independence of the adsorption capacity on the pH.

For the initial extremely acid and basic (2 and 12) pH values, the final pH of RB solution has not changed much (from 2 to 2.5 and from 12 to 11). This may explain the reduction of the retention rate from 85% to 83%.

3.7. Study of the adsorption kinetics

A kinetic study is needed in the determination of the adsorption rate constants, the equilibrium adsorption capacity, and the adsorption mechanism. Three models were tested for four RB initial concentrations of (50, 100, 200, and 400 mg/L) at a constant temperature of 20°C.

3.7.1. Pseudo-first-order models

The Lagergren pseudo-first-order model (PFOM) is expressed as follows [43]:

$$\ln(Q_e - Q_t) = \ln Q_e - K_1 \cdot t \quad (3)$$

where K_1 (min⁻¹) is the pseudo-first-order adsorption kinetics rate constant, Q_t is the adsorption capacity at time t and Q_e is the adsorption capacity at equilibrium.

The values of Q_e and K_1 for the pseudo-first-order kinetic model were determined from the intercepts and the slopes of the plots of $\ln(Q_e - Q_t)$ vs. time (Fig. 9a). The correlation factor, K_1 , and Q_e values (experimental and calculated) are shown in Table 4.

3.7.2. Pseudo-second-order model

The pseudo-second-order (PSOM) model is given as follows [44]:

$$\frac{t}{Q_t} = \frac{1}{K_2 \cdot Q_e^2} + \frac{1}{Q_e^2} t \quad (4)$$

where K_2 is the second-order adsorption kinetics rate constant.

The values of Q_e and K_2 were determined from the slopes and intercepts of the plot of t/Q_t vs. time (Fig. 9b).

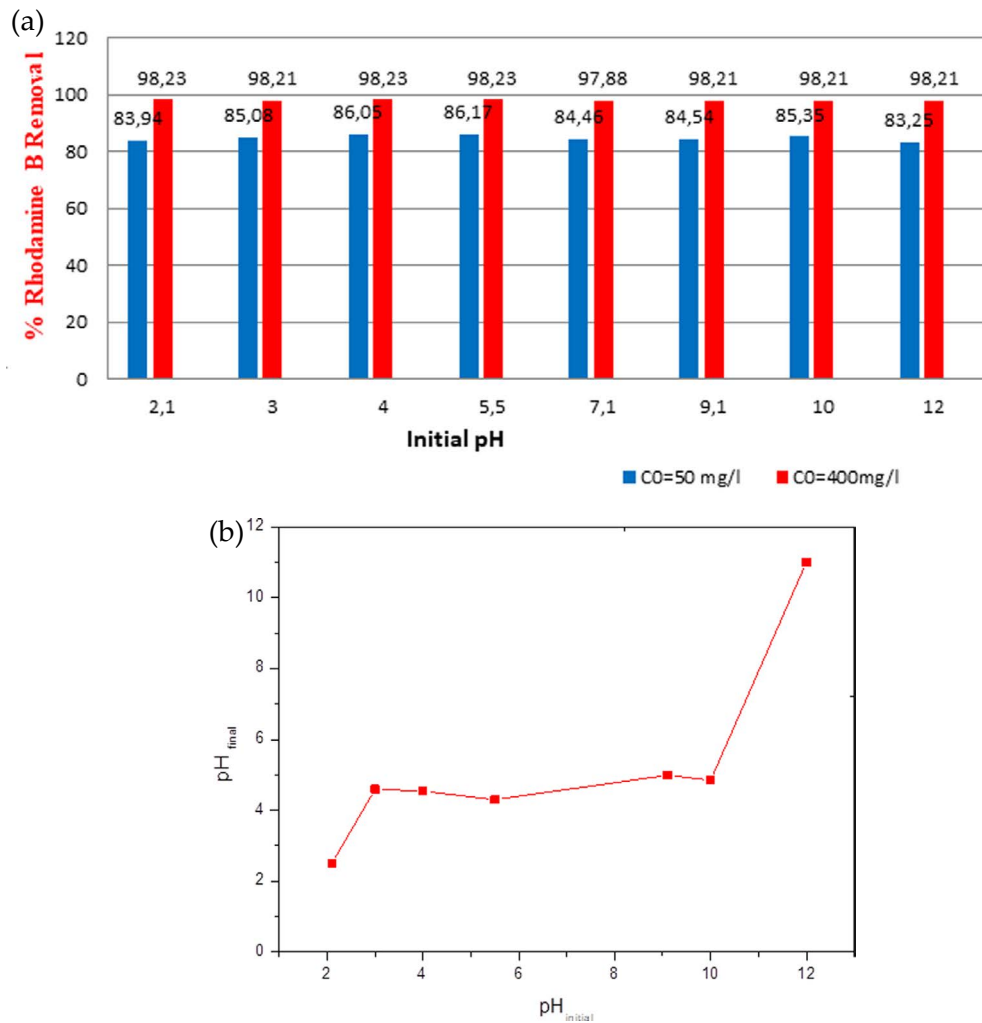


Fig. 8. (a) Effect of pH on removal efficiency of Rhodamine B and (b) final pH of Rhodamine B solution.

The results are shown in Table 3 along with the corresponding correlation factors.

3.8. Adsorption mechanism

3.8.1. Intraparticle diffusional model

When diffusion of dye molecules inside the internal adsorbent surface is the rate-limiting step, then data can be represented by the following equation:

$$Q_t = K_{\text{int}} t^{(1/2)} \quad (5)$$

where K_{int} ($\text{mg/g min}^{1/2}$) is the rate constant for adsorption kinetics of intraparticle diffusional model (IDM) and can be directly calculated from the slope of the regression line.

3.8.2. Boyd model

To determine the limiting step of adsorption kinetics, Boyd has proposed a model based on the assumption that intraparticle diffusion is the only limiting step controlling the process, which is expressed as follows [38]:

$$F = 1 - \frac{6}{\tau^2} \exp(-B_t) \quad (6)$$

where F is the fraction of solute adsorbed at different time t and B_t is a mathematical function of F and given by [45]:

$$B_t = -0.4977 - 2.303 \log(1 - F) \quad (7)$$

$$F = \frac{Q_t}{Q_e} \quad (8)$$

Boyd state that if the plot of B_t is linear and passes through the origin then pore diffusion controls the rate of mass transfer. If the plot is nonlinear or linear but does not pass through the origin, then it is concluded that the transport is extraparticle (external diffusion).

From the linear regression tests shown in Fig. 9b, it can be concluded that retention of RhB by the BP was better represented by a second-order kinetics and it showed an excellent linearity compared to the plots from the pseudo-first-order equation (Fig. 9a) as well as high levels of congruence with the data. As already mentioned above and at

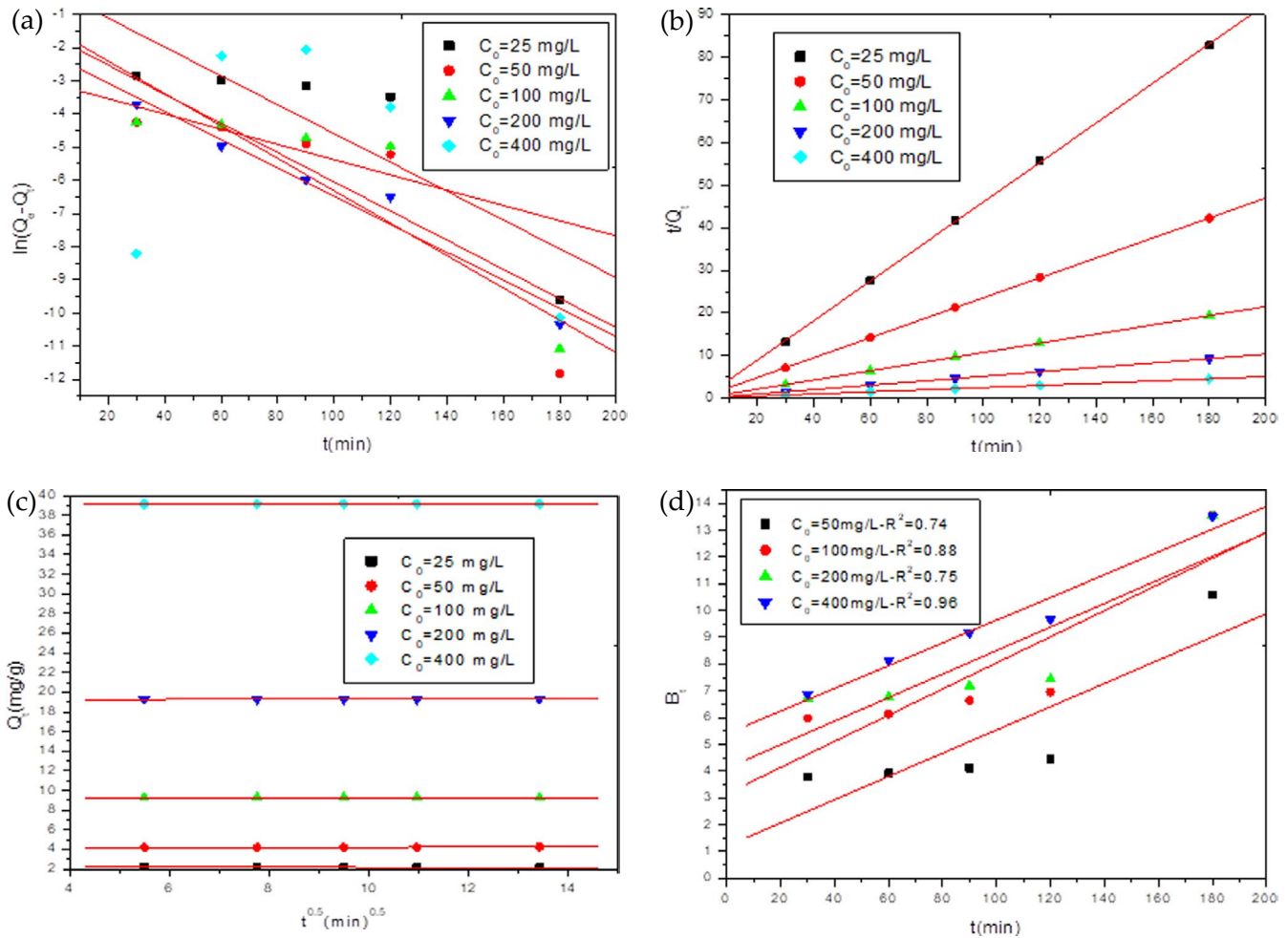


Fig. 9. Test of (a) pseudo-first-order and (b) pseudo-second-order equation for RhB onto BP. Test of (c) intraparticle diffusional and (d) Boyd's equation for RhB onto BP.

a given initial solute concentration, the retention capacity seemed to be time independent and therefore the representing lines of Q_e vs. t did not go through the origin excluding IDM which could not be the rate-limiting step of adsorption phenomena [46], as confirmed by Boyd model. Since the plot of B_t vs. t (Fig. 9c) does not pass through the origin, it was suggested that initially, the diffusional film controlled the adsorption process, the mechanism was complex, and the model was not involved in the rate-controlling [47].

From the parameters shown in Table 3, the highest correlation coefficient ($R^2 > 0.999$) for different initial dye concentrations correspond to second-order model; also the experimental Q_{exp} values were in agreement with the calculated Q_{cal} values obtained from the linear plots where the values of the rate constant K_2 were found to increase from 1.16 to 52.27 (g/mg min) for an increase in the initial concentration from 50 to 400 mg/L. This confirmed the experimental results. Yagub et al. [48] have found that the kinetic adsorption data of dye is usually better represented by a PSOM for most adsorption systems and even for heavy metals in nanomaterials such as Mercury(II) by EDTA-functionalized magnetic $CoFe_2O_4@SiO_2$ and core-shell structure [49,50].

3.9. Adsorption equilibrium isotherm

The equilibrium adsorption isotherm is important in the design of adsorption system. In order to define the type of adsorption isotherm, the amount of RB adsorbed at equilibrium was followed as a function of the concentration of the solution at equilibrium, an initial concentration ranges were 2–400 mg/L. According to Charles and Hill classification, the curve shown in Fig. 10 is a typically “S” type class (S3) isotherm and is characterized by a vertical orientation of adsorbed molecules at the surface [51].

This curve is usually obtained in the case of strong competition between the adsorbate and solvent molecules for substrate sites, particularly on polar surface, similarly to the case of phenol in an aqueous solution in contact with alumina as adsorbent [52]. This is a good agreement with the studied system RB-water-BP and can explain the high capacity of a non-active and less porous substrate BP with a low specific surface area.

The mathematical interpretation of the adsorption isotherms is performed using the most frequent models such as Langmuir, Freundlich, Temkin, and BET models. The expression of each model is as follows:

Table 3
Kinetic parameters for the adsorption of Rhodamine B onto BP adsorbent

Models	Rhodamine				
	25 mg/L	50 mg/L	100 mg/L	200 mg/L	400 mg/L
Q_{exp} (mg/g)	2.1762	4.2647	9.2853	19.2858	39.1535
PFOM					
K_1 (min ⁻¹)	-0.0299	0.0434	0.0488	0.0439	0.0424
R^2	0.4043	0.7370	0.7687	0.7515	0.9604
q_{calc}	0.04591	0.7820	0.2385	0.1923	0.10768
PSOM					
K_2 (g/mg min)	1.4177	1.1603	11.4468	22.5217	52.2701
R^2	0.9996	0.9998	1	1	1
q_{calc}	2.1569	4.2769	9.2885	19.2901	39.1543
IDM					
K_{int} (mg/g min)	-0.01251	0.0073	0.0018	0.0018	0.0029
R^2	0.4978	0.9183	0.9387	0.9387	0.7468

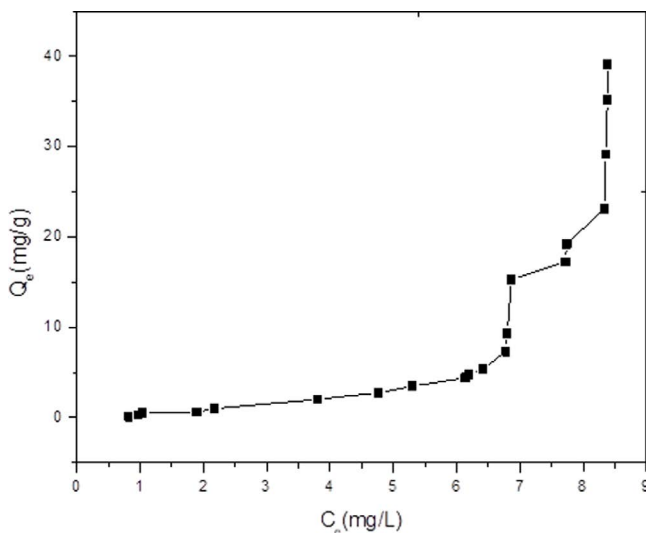


Fig. 10. Adsorption isotherm of RB onto BP.

- The Langmuir isotherm model is expressed by Eq. (9) and has been applied to describe the adsorption of dyes onto different materials [53].

$$q_e = \frac{Q_m b C_e}{1 + b C_e} \quad (9)$$

The linearized form is as:

$$q_e = -\frac{1}{b} \frac{q_e}{C_e} + b Q_m \quad (10)$$

where q_m is the maximum adsorption capacity of RhB (mg/g) and b is the equilibrium constant related to the adsorption energy (L/mg). The linear plots of q_e vs. q_e/C_e showed that the adsorption is not represented by Langmuir isotherm;

because the Q_m and b which were determined from the slopes and intercepts of the respective plots have a negative value and are listed in Table 4.

- Freundlich isotherm model was also used for RhB data to test the possibility of non-ideal adsorption onto heterogeneous surfaces [54]. Freundlich isotherm can be obtained assuming a logarithmic decrease in enthalpy of adsorption with the increase in the fraction of occupied sites and is commonly given by the following equation [55]:

$$q_e = K C_e^{1/n} \quad (11)$$

Eq. (11) can be linearized in the logarithmic form shown by Eq. (12) from which the Freundlich constants can be determined as [56]:

$$\ln q_e = \ln K + \frac{1}{n} \ln C_e \quad (12)$$

with q_e is the amount adsorbed per unit mass of the adsorbent, C_e is the equilibrium concentration, $1/n$ and K are constants.

Constant K shows the degree of adsorption while n represents the intensity of the adsorption [57].

The linear plots of $\ln q_e$ vs. $\ln C_e$ showed that the adsorption is well-represented by Freundlich isotherm, as shown in Table 4 with a correlation coefficient value $R^2 = 0.90179$. Indicated that this adsorption process involved a heterogeneous adsorbent surface.

- Temkin isotherm considered the effects of some indirect adsorbate interactions on adsorption isotherms and suggested that they might induce a linear decrease of the heat of adsorption of all the molecules in the layer with coverage [58]. The Temkin isotherm has been commonly applied in the following form:

Table 4
Parameters for the equilibrium models of Rhodamine B

Models	Parameters			
Langmuir	$Q_m = -1.3929$ mg/g	$b = -0.1417$	$R = 0.8775$	$R^2 = 0.7700$
Freundlich	$n = 0.21578$	$K_f = 0.49108$	0.94963	$R^2 = 0.90179$
Temkin	$A_T = 0.67201069$	$B_T = 16.350017$	0.65036	$R^2 = 0.42296$
BET	$Q_m = 40.749796$ mg/g	$C = -0.0341797$	0.88988	$R^2 = 0.79188$

$$q_e = \frac{RT}{b_T} \ln(A_T C_e) \tag{13}$$

Or in the linear form as:

$$q_e = B_T \ln A_T + B_T \ln C_e \tag{14}$$

with B_T and A_T are the Temkin isotherm constants and B is related to the heat of adsorption. The linear isotherm constants and coefficients were determined by the plots of q_e vs. $\ln C_e$ and the obtained values are shown in Table 4; from the value of R^2 obtained ($R^2 = 0.42296$), we can conclude that this isotherm cannot explain the experimental data.

- BET models assumed that a number of layers of adsorbate molecules form at the surface of the adsorbent and that the Langmuir equation is applied to each layer of adsorption and is expressed as [59]:

$$q_e = \frac{KQ_m \left(\frac{C}{C_0}\right)}{\left(1 - \frac{C}{C_0}\right) \left[1 + (K-1) \frac{C}{C_0}\right]} \tag{15}$$

where Q_m is the maximum adsorption capacity of RhB (mg/g), K is constant BET, and C_0 is the initial concentration of Rhodamine (mg/L).

The theoretical parameters of adsorption isotherms along with regression coefficients are listed in Table 4. According to the corresponding R^2 value of 0.7919, the BET model can be regarded as not adequate. However, the obtained $Q_m = 40.7498$ mg/g was close to the experimental value of 39.16 mg/g, indicating that the RhB molecules are rather adsorbed in multilayers in agreement with Langmuir S model, describing cooperative adsorption characterized by interactions between adsorbates or between adsorbate and adsorbent called “co-operative adsorption” [52]. Also, the calculations led to a nonphysical negative value of the adsorption capacity Q_m , indicating that the Langmuir model was not suitable at all.

4. Conclusion

The present study showed clearly how household food wastes like bean peels (BP) can be valorized as performing adsorbents to remove pollutants like RhB from wastewaters effluents mainly from textile industries.

The considered bean peels adsorbent material was characterized by means of various techniques, focusing mainly on its surface properties.

In fact, the determination of the pH of the point of zero charges of the BP solid support BP in the natural state was 6.2. Consequently below this value, the surface was positively charged whereas above it had a negative charge. The titration of BP surface the sites, showed that the surface contained at the same time acid and basic groups, simultaneously, insinuating a polar surface of BP. However, the specific surface calculated by the application of the BET linear equation was very low ($S_{BET} = 0.4213$ m²/g) and the total pore volume was equal to 1.523×10^{-3} cm³/g.

The experimental results led to useful results like the non-influence of the pH on the BP adsorption capacity, due to the amphoteric nature of the surface.

The measurements of the kinetics of sorption have shown that the adsorption process followed the PSOM confirmed by q_{calc} and R^2 values.

The adsorption isotherm was of an S type and was well-represented by the Freundlich model.

Finally, all the obtained results enable to conclude that the adsorbent material made out of bean peels can be effectively be regarded as a good adsorbent for a zwitteric molecule like that of RhB, in addition of being cheap and abundant. It does not require any extensive pretreatment, just a simple washing with distilled water which provides a polar surface with also an amphoteric character. Further, developments should be carried out in order to extend its use to wastewaters treatments issuing from industries like the textile ones.

References

- [1] M.R. Singh, A. Gupta, Water Pollution Sources: Effects and Control, Pointer Publishers, Jaipur, 2016.
- [2] S.S. Vieira, Z.M. Magriotis, N.A.V. Santos, M.d.G. Cardoso, A.A. Saczk, Macauba palm (*Acrocomia aculeata*) cake from biodiesel processing: an efficient and low cost substrate for the adsorption of dyes, Chem. Eng. J., 183 (2012) 152–161.
- [3] K.A. Adegoke, O.S. Bello, Dye sequestration using agricultural wastes as adsorbents, Water Resour. Ind., 12 (2015) 8–24.
- [4] A. Ashfaq, A. Khatoun, Waste management of textiles: a solution to the environmental pollution, Int. J. Curr. Microbiol. Appl. Sci., 3 (2014) 780–787.
- [5] N. Mohan, N. Balasubramanian, C.A. Basha, Electrochemical oxidation of textile wastewater and its reuse, J. Hazard. Mater., 147 (2007) 644–651.
- [6] H.-L. Kim, J.-B. Cho, Y.J. Park, I.H. Cho, Treatment and toxicity reduction of textile dyeing wastewater using the electrocoagulation-electroflotation process, J. Environ. Sci. Health., Part A Toxic/Hazard. Subst. Environ. Eng., 8 (2016) 661–668.

- [7] S. Meric, H. Selcuk, V. Belgiorno, Acute toxicity removal in textile finishing wastewater by Fenton's oxidation: ozone and coagulation–flocculation processes, *Water Res.*, 39 (2005) 1147–1153.
- [8] M. Vinuth, H.S. Bhojya Naik, B.M. Vinoda, S.M. Pradeepa, A.G. Kumar, K.G. Sekhar, Rapid removal of hazardous rose bengal dye using Fe(III)–montmorillonite as an effective adsorbent in aqueous solution, *J. Environ. Anal. Toxicol.*, 6 (2016) 1–7.
- [9] L. Rizzo, H. Selcuk, A.D. Nikolaou, S.M. Pagano, V. Belgiorno, A comparative evaluation of ozonation and heterogeneous photocatalytic oxidation processes for reuse of secondary treated urban wastewater, *Desal. Water Treat.*, 52 (2014) 1414–1421.
- [10] M.K. Nizam Mahmud, M. Remy Rozainy, M.A.Z. Ismail Abustan, N. Baharun, Electrocoagulation process by using aluminium and stainless steel electrodes to treat total chromium, colour and turbidity, *Procedia Chem.*, 19 (2016) 681–688.
- [11] M.C. Somase Kharara Reddy, V. Nirmala, Bengal gram seed husk as an adsorbent for the removal of dyes from aqueous solutions – equilibrium studies, *Arabian J. Chem.*, 9 (2013) 1695–1706.
- [12] R. Malik, D.S. Ramteke, S.R. Wate, Adsorption of malachite green on groundnut shell waste based powdered activated carbon, *Waste Manage.*, 27 (2007) 1129–1138.
- [13] T. Robinson, G. McMullan, R. Marchant, P. Nigam, Remediation of dyes in textile effluent: a critical review on current treatment technologies with a proposed alternative, *Bioresour. Technol.*, 77 (2001) 247–255.
- [14] A. Bhatnagar, M. Sillanpää, A. Witek-Krowiak, Agricultural waste peels as versatile biomass for water purification, *Chem. Eng. J.*, 270 (2015) 244–271.
- [15] R.K. Gautm, A. Mudhoo, G. Lofrano, M.C. Chattopadhyaya, Biomass-derived biosorbents for metal ions sequestration: adsorbent modification and activation methods and adsorbent regeneration, *J. Environ. Chem. Eng.*, 2 (2014) 239–259.
- [16] S. De Gisi, G. Lofrano, M. Grassi, M. Notarnicola, Characteristics and adsorption capacities of low-cost sorbents for wastewater treatment, *Sustainable Mater. Technol.*, 9 (2016) 10–40.
- [17] J.F. Duarte Neto, I.D.S. Pereira, V.C. da Silva, H.C. Ferreira, G.d.A. Neves, R.R. Menezes, Study of equilibrium and kinetic adsorption of Rhodamine B onto purified bentonite clays, *Cerâmica*, 64 (2018) 598–607.
- [18] G. Cinelli, F. Cuomo, L. Ambrosone, M. Colella, A. Ceglie, F. Venditti, F. Lopez, Photocatalytic degradation of a model textile dye using carbon-doped titanium dioxide and visible light, *J. Water Process. Eng.*, 20 (2017) 71–77.
- [19] D. Tan, B. Bai, D. Jiang, L. Shi, S. Cheng, D. Tao, S. Ji, Rhodamine B induces long nucleoplasmic bridges and other nuclear anomalies in *Allium cepa* root tip cells, *Environ. Sci. Pollut. Res. Int.*, 21 (2014) 3363–3370.
- [20] F. López Arbeloa, A. Costela, I. López Arbeloa, Molecular structure effects on the lasing properties of Rhodamines, *J. Photochem. Photobiol., A*, 55 (1990) 97–103.
- [21] M.V. Lopez-Ramon, F. Stoeckli, C. Moreno-Castilla, F. Carrasco-Marinn, On the characterization of acidic and basic surface sites on carbons by various techniques, *Carbon*, 37 (1999) 1215–1221.
- [22] N. Marnier, J. Dumonceau, J. Chupeau, F. Fromage, Etude expérimentale et modélisation de la sorption des ions lanthanides trivalents sur l'hématite, *C.R. Acad. Sci.*, 317 (1993) 311–317.
- [23] N. Marnier, A. Delisée, F. Fromage, Surface complexation modelling of Yb(III) and Cs(I) sorption on silica, *J. Colloid Interface Sci.*, 212 (1999) 228–233.
- [24] H. Yang, R. Yan, D.H. Lee, C. Zheng, Characteristics of hemicellulose, cellulose and lignin pyrolysis, *Fuel*, 86 (2007) 1781–1788.
- [25] E. Raymundo-Pinero, P. Azaïs, T. Cacciaguerra, D. Cazorla-Amoro, A. Linares-Solano, F. Béguin, KOH and NaOH activation mechanisms of multiwalled carbon nanotubes with different structural organisation, *Carbon*, 43 (2005) 786–795.
- [26] O.S. Bello, E.O. Alabi, K.A. Adegoke, S.A. Adegboyega, A.A. Inyinbor, A.O. Dada, Rhodamine B dye sequestration using *Gmelina aborea* leaf powder, *Heliyon*, 5 (2019) 02872 1–12, doi: 10.1016/j.heliyon.2019.e02872.
- [27] N. Marnier, J. Dumonceau, J. Chupeau, F. Fromage, Modeling of Yb(III) sorption on kaolinite by using single oxide, *C.R. Acad. Sci.*, 318 (1994) 177–183.
- [28] N. Marnier, J. Dumonceau, J. Chupeau, F. Fromage, Comparative study of trivalent lanthanide ions sorption on hématite and goethite, *C.R. Acad. Sci.*, 317 (1993) 1561–1567.
- [29] F. Ahnert, H.A. Arafat, N.G. Pinto, A study of the influence of hydrophobicity of activated carbon on the adsorption equilibrium of aromatics in non-aqueous media, *Adsorption*, 9 (2003) 311–319.
- [30] A. Ozer, G. Dursun, Removal of methylene blue from aqueous solution by dehydrated wheat bran carbon, *J. Hazard. Mater.*, 146 (2007) 262–269.
- [31] J. Sahar, A. Naeem, M. Farooq, S. Zareen, F.S. Sherazi, Kinetic studies of graphene oxide towards the removal of Rhodamine B and congo red, *Int. J. Environ. Anal. Chem.*, 99 (2019) 1–14, doi: 10.1080/03067319.2019.1679802.
- [32] R. Khalighi Sheshdeh, M.R.N. Khosravi, K. Badii, N.Y. Limaee, G. Golkarnareni, Equilibrium and kinetics studies for the adsorption of Basic Red 46 on nickel oxide nanoparticles-modified diatomite in aqueous solutions, *J. Taiwan Inst. Chem. Eng.*, 45 (2014) 1792–1802.
- [33] H. Ali, S.K. Muhammad, Biosorption of Crystal violet from water on leaf biomass of *Calotropis procera*, *J. Environ. Sci. Technol.*, 1 (2008) 143–150.
- [34] P. Senthil Kumar, S. Ramalingam, C. Senthamarai, M. Niranjanaa, P. Vijayalakshmi, S. Sivanesan, Adsorption of dye from aqueous solution by cashew nut shell: studies on equilibrium isotherm, kinetics and thermodynamics of interactions, *Desalination*, 261 (2010) 52–60.
- [35] M.-F. Hou, C.-X. Mac, W.-D. Zhang, X.-Y. Tang, Y.-N. Fan, H.-F. Wan, Removal of Rhodamine B using iron-pillared bentonite, *J. Hazard. Mater.*, 186 (2011) 1118–1123.
- [36] Y. Goto, Y. Nema, K. Matsuoka, Removal of Zwitterionic Rhodamine B using foam separation, *J. Oleo Sci.*, 69 (2020) 563–567.
- [37] V.S. Nguyen, K.C. Dang, Removal of Rhodamine B from aqueous solution via adsorption onto microwave activated rice husk ash, *J. Dispersion Sci. Technol.*, 38 (2017) 216–222.
- [38] E.K.G. Guechi, Equilibrium, kinetics and mechanism for the removal of Rhodamine B by adsorption on Okoume (*Aucoumea klaineana*) sawdust from aqueous media, *Desal. Water Treat.*, 94 (2017) 164–173.
- [39] C. Namasivayam, R.T. Yamuna, Removal of Rhodamine-B by biogas waste slurry from aqueous solution, *Water Air Soil Pollut.*, 65 (1992) 101–109.
- [40] H. Lata, S. Mor, V.K. Garg, R.K. Gupta, Removal of a dye from simulated wastewater by adsorption using treated parthenium biomass, *J. Hazard. Mater.*, 153 (2008) 213–220.
- [41] T. Smitha, T. Santhi, A.L. Prasad, S. Manonmani, *Cucumis sativus* used as adsorbent for the removal of dyes from aqueous solution, *Arabian J. Chem.*, 10 (2017) S244–S251.
- [42] J. Shah, M.R. Jan, A. Haq, Y. Khan, Removal of Rhodamine B from aqueous solutions and wastewater by walnut shells, *Front. Chem. Sci. Eng.*, 7 (2013) 428–436.
- [43] D. Sarkar, D.K. Chattoraj, Activation parameters for kinetics of protein at silica–water interface, *J. Colloid Interface Sci.*, 157 (1999) 1179–1204.
- [44] F.C. Wu, R.L. Tseng, R.S. Juang, Kinetics of colour removal by adsorption from water using activated clay, *Environ. Technol.*, 22 (2001) 721–729.
- [45] H.M.H. Gad, A.A. El-Sayed, Activated carbon from agricultural by-products for the removal of Rhodamine-B from aqueous solution, *J. Hazard. Mater.*, 168 (2009) 1070–1081.
- [46] G. Crini, H.N. Peindy, F. Gimbert, C. Robert, Removal of CI Basic Green 4 (Malachite Green) from aqueous solutions by adsorption using cyclodextrin based adsorbent: kinetic and equilibrium studies, *Sep. Purif. Technol.*, 53 (2007) 97–110.
- [47] Z. Zeng, X. Tan, Y. Liu, S. Tian, G. Zeng, L. Jiang, S. Liu, J. Li, N. Liu, Z. Yin, Comprehensive adsorption studies of doxycycline and ciprofloxacin antibiotics by biochars prepared at different

- temperatures, *Front. Chem.*, 6 (2018) 1–11, doi: 10.3389/fchem.2018.00080.
- [48] M.T. Yagub, T.K. Sen, S. Afroze, H.M. Ang, Dye and its removal from aqueous solution by adsorption, *Adv. Colloid Interface Sci.*, 209 (2014) 172–184.
- [49] K. Xia, Y. Guo, Q. Shao, Q. Zan, R. Bai, Removal of Mercury(II) by EDTA-functionalized magnetic $\text{CoFe}_2\text{O}_4/\text{SiO}_2$ nanomaterial with core-shell structure, *Nanomaterials*, 9 (2019) 1–23, doi: 10.3390/nano9111532.
- [50] Z. Zhang, K. Xia, Z. Pan, C. Yang, X. Wang, G. Zhana, Y. Guo, R. Bai, Removal of mercury by magnetic nanomaterial with bifunctional groups and core-shell structure: synthesis, characterization and optimization of adsorption parameters, *Appl. Surf. Sci.*, 500 (2020) 1–14, doi: 10.1016/j.apsusc.2019.143970.
- [51] C.H. Giles, D. Smith, A. Huiston, A general treatment and classification of the solute adsorption isotherm, *J. Colloid Interface Sci.*, 47 (1974) 755–765.
- [52] C.H. Giles, T.H. Mac Ewan, S.N. Nakhwa, D. Smith, A system of classification of solution adsorption isotherms, and its use in diagnosis of adsorption mechanisms and in measurement of specific surface areas of solids, *Stud. Adsorpt.*, 11 (1960) 3973–3993.
- [53] V. Vimonses, S.M. Lei, B. Jin, C.W.K. Chowd, C. Saint, Kinetic study and equilibrium isotherm analysis of Congo Red adsorption by clay materials, *Chem. Eng. J.*, 148 (2009) 354–364.
- [54] H. Freundlich, Over the adsorption in solution, *J. Phys. Chem.*, 57 (1906) 358–471.
- [55] N. Bhullar, K. Kumari, D. Sud, A biopolymer-based composite hydrogel for Rhodamine 6G dye removal: its synthesis, adsorption isotherms and kinetics, *Iran. Polym. J.*, 27 (2018) 527–535.
- [56] J. Gülen, F. Zorbay, Methylene blue adsorption on a low cost adsorbent – carbonized peanut shell, *Water Environ. Res.*, 89 (2017) 805–816.
- [57] H. Tahir, M. Sultan, N. Akhtar, U. Hameed, T. Abid, Application of natural and modified sugar cane bagasse for the removal of dye from aqueous solution, *J. Saudi Chem. Soc.*, 20 (2016) 115–121.
- [58] G. Akkaya, A. Ozer, Biosorption of Acid Red 274 (AR 274) on *Dicranella varia*: determination of equilibrium and kinetic model parameters, *Process Biochem.*, 40 (2005) 3559–3568.
- [59] Z. Al-Qodah, R. Shawabkha, Production and characterization of granular activated carbon from activated sludge, *Braz. J. Chem. Eng.*, 26 (2009) 127–136.